ChemComm

COMMUNICATION

View Article Online
View Journal | View Issue

Cite this: *Chem. Commun.*, 2022, 58, 9210

Received 16th March 2022,
Accepted 18th July 2022

DOI: 10.1039/d2cc01515c

rsc.li/chemcomm

A unique water soluble probe for measuring the cardiac marker homocysteine and its clinical validation†

Snehasish Debnath,[ab] Ratish R. Nair,[ab] Riya Ghosh,[ab] Gaddam Kiranmai,[c] Narsini Radhakishan,[d] Narayana Nagesh *[c] and Pabitra B. Chatterjee *[ab]

A series of copper(II) compounds 1–4 were synthesized and developed as fluorogenic probes to measure the cardiac marker homocysteine (Hcy) without any interference from other bioanalytes prevalent in human blood plasma including, cysteine and glutathione. UV-vis and EPR studies have provided confirmatory evidence for reduction-induced-emission-enhancement of the probe, which is responsible for the observed "off-to-on" behaviour towards Hcy. Water solubility, remarkable fluorescence enhancement (55–111 fold), and low detection ability (nearly 2.5 μM) make the probe suitable for clinical testing of cardiac samples. Investigation of 1 against a few reductive interferents testifies its specificity for Hcy. Results from clinical examination of cardiac samples by 1 when combined with the outcome of the reliability testing involving a clinically approved commercial immunoassay kit, validates the prospect of the molecular probe for direct measurement of Hcy in human plasma, which is unprecedented.

High concentrations (>15 μM) of the cardiac marker homocysteine (Hcy, Scheme S1, ESI†) in human plasma are accompanied by the early onset of several critical health illnesses and age related pathologies *viz.* atherosclerosis and thrombosis, acute coronary heart disease, ischemic stroke, early pregnancy loss, chronic renal dysfunction, microalbuminuria, cognitive impairment, Alzheimer's disease, and Parkinson's disease.[1] Consequently, measurement of plasma total homocysteine (tHcy) is obligatory for clinical supervision of various pathologies. Despite tens of thousands of publications in the literature on the relationship between Hcy and above-mentioned health disorders, very few Hcy selective optical probes exist in the literature.[2] Ever since Strongin *et al.* reported the optical method for selective detection of Hcy,[2a] not many reports are documented in the literature describing interference-free optical detection of Hcy (Table S1, ESI†). As clearly pointed out by Strongin and co-workers,[3] the obligatory requirement of non-aqueous media for the detection purpose has presumably made the clinical application of the Hcy-specific optical probes challenging. Wang *et al.* have recently developed a BODIPY-based complex for selective detection of Hcy in an aqueous medium.[2e] However, synthetic difficulty, cost of the reagents (*i.e.* BODIPY), and lack of detailed clinical validation and testing could be a major limitation in the development of optical assays using Wang's probe.[2e]

In this communication, we report the synthesis and characterization of four water-soluble (100% aqueous) copper compounds (**1–4**) to develop optical probes for measuring Hcy directly and selectively, in clinical samples. Upon addition of Hcy, non-fluorescent **1–4** showed 55–111 fold emission enhancement at physiological pH conditions, without any interference. Mechanistic studies have provided evidence for the preferential affinity of **1–4** towards Hcy. Herein, we demonstrate clinical testing of the Hcy-specific optical probe in a large number of human samples (cardiac patients and healthy volunteers as well). The performance of our presented assay has also been tested with a clinically approved immunoassay kit involving 60 clinical samples, which is unprecedented in the literature.

Yellow solids of the ligands HL_1–HL_4 were prepared from 7-hydroxycoumarin, as described in Scheme S2 (ESI†). The purity and molecular structures of HL_1–HL_4 and copper complexes (**1–4**) were established by C/H/N, IR, NMR, and ESI-MS (Fig. S1–S17, ESI†). Structural confirmation was gained from single crystal X-ray analyses (Fig. 1a and Fig. S13, Tables S2 and S3, ESI†). The structural index parameter τ (= 0.07), determined from the equation $\tau = (\beta - \alpha)/60$ (wherein, β and α are the two largest *L*–M–*L* angles),[4] indicates the square pyramidal geometry of the copper complex. Water-soluble 1–4 showed two weak absorption peaks as shoulders at 410 and 365 nm (Fig. S18, ESI†).

[a] *Analytical & Environmental Science Division and Centralized Instrument Facility, CSIR-CSMCRI, G. B. Marg, Bhavnagar, Gujarat, India. E-mail: pbchatterjee@csmcri.res.in*
[b] *Academy of Scientific and Innovative Research (AcSIR), Ghaziabad 201002, India*
[c] *Medical Biotechnology Complex, CSIR-CCMB, ANNEXE II, Hyderabad, Telangana, India. E-mail: nagesh@ccmb.res.in*
[d] *Department of Biochemistry, Nizam's Institute of Medical Sciences, Punjagutta, Hyderabad, Telangana, India*

† Electronic supplementary information (ESI) available: Materials and methods, synthesis, characterization data, Fig. S1–S53, Schemes S1–S3 and Tables S1–S7. CCDC 2105918–2105921. For ESI and crystallographic data in CIF or other electronic format see DOI: https://doi.org/10.1039/d2cc01515c

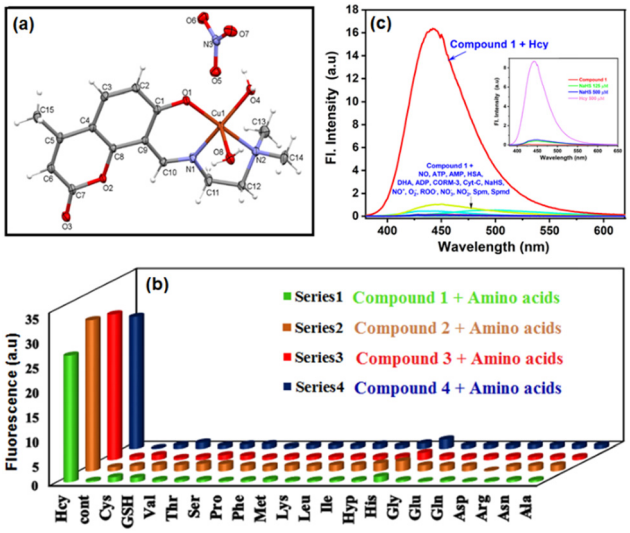

Fig. 1 (a) ORTEP view and atom-numbering scheme of the copper compound 1. (b) Fluorimetric responses of **1–4** (20 μM) toward different amino acids upon excitation at 370 nm in aqueous HEPES buffer solution (10 mM) at physiological pH (7.4). (c) Fluorescence responses of **1** (20 μM) towards other biologically relevant species (125 μM). Inset: Fluorescence of **1** (20 μM) towards variable concentrations of NaHS.

Furthermore, the complex displayed a d–d band at 625 nm (ε, 160 L mol^{-1} cm^{-1}). Because of the unique physical properties, high quantum yield, and great binding ability towards various analytes, coumarin derivatives have been found as fantastic fluorophores in the literature.[5] As a result of C=N isomerisation and/or electron transfer processes,[6] HL_1–HL_4 are weakly fluorescent (Φ_f = 0.01–0.014). However, complexes **1–4** are non-luminescent. The high binding affinity of Cu^{2+} towards ONN donor sites of HL_1–HL_4 further restricts the hydrolysis of 1–4 at neutral pH,[7] which has been confirmed from the pH profile (*vide infra*).

Emission behaviour of **1–4** against different amino acids is shown in Fig. 1b and Fig. S19 (ESI†), which revealed a large luminescence enhancement upon addition of Hcy with the formation of cyan colour (Fig. S20, ESI†). To check the efficacy of the probes for clinical applications, pH-variable luminescence measurement of **1–4** was explored further (Fig. S21–S24, ESI†). Throughout the pH regime, **1–4** remained non-fluorescent. To our surprise, emission spectra of **1–4** with Hcy showed maximum fluorescence at physiological pH. Hence, the working pH was found to be 6.5–8 (Fig. S21–S24, ESI†). All spectral experiments were performed with aqueous HEPES buffer (100% water) at physiological pH. We further have investigated the time-response behaviour of **1** in presence of Hcy. Results shown in Fig. S25 (ESI†), discloses that the luminescence intensity of **1** reaches a maximum within 60–70 min incubation with Hcy. Cys initially shows a little turn-on response. However, after 7–8 min incubation, the solution turned non-fluorescent. Luminescence spectra of **1–4** were measured after incubation of the probes with various amino acids and GSH for 30 min. A sharp 55–111 fold fluorescence increase was observed with Hcy. Thus, demonstrating Hcy selective nature of **1–4**. The quantum yields were estimated to be within 0.134 to 0.091, much higher than the ligands. Thus, indicating adduct formation between Hcy and probes, instead of the replacement of the iminocoumarin ligand from the probes. From the Job's plot, the binding stoichiometry was found to be 1 : 1 (Fig. S26, ESI†). Without any interference, **1–4** responded to Hcy, even in presence of Cys and GSH (Fig. S27–S30, ESI†). Interference of Hcy congeners, *i.e.* Cys and GSH, have also been tested in different stoichiometric mixtures of them with Hcy. Results displayed in Fig. S31 (ESI†) reveals non-interference from Cys and GSH during the detection of Hcy. From fluorescence titration (Fig. S32–S35, ESI†), the calculated binding constants were found to be in the range 1.23–2.15 × 10^3 M^{-1} (Fig. S36, ESI†). The limit of detection (LOD) was calculated (Fig. S37, ESI†) to be in the order of 2.5 μM (compound **2**), which is below the normal level of Hcy in healthy human blood plasma. Linearity within 0–100 μM supports the suitability of **1–4** at low concentration. Remarkable specificity of the probe towards Hcy is further reinforced when **1** was screened against a range of important bioanalytes (Fig. 1c). Furthermore, using varying concentrations of NaHS and other sulfur containing interferents that are commonly present in blood plasma, the non-emissive nature of the probe did not change (inset, Fig. 1c and Fig. S38, ESI†).

Reversible detection of Hcy by the probes (Fig. S39, ESI†) clearly demonstrates that the displacement of the ligand by the incoming Hcy ligand is not happening in **1–4**. Thus, not in line to the proposal of Kim *et al.*[7] This could be the result of the redox reaction between probe and Hcy, wherein, Hcy reduces Cu(II) to Cu(I) at physiological pH. Upon deprotonation, Hcy binds Cu(I). Therefore, a ternary Cu(I) complex is formed. ESI-MS of **1**, when recorded after half an hour of incubation with Hcy, showed a molecular ion peak of the intermediate ternary species at m/z = 512.58. This clearly implies the formation of the intermediate Cu(I) species, as shown in Fig. S40 (ESI†). Presumably, the reduction of Cu(II) is responsible for the fluorimetric "off-to-on" responses of **1–4** with Hcy. On the contrary, Cys with one less methylene group (Scheme S1, ESI†), initially showed a turn on response, which quickly diminished over time. After 7–8 min incubation, the solution mixture quenched completely. The pK_a value of the sulfhydryl group of Cys (8.00) is lower than that of Hcy (8.87).[8] As a result, Cys deprotonates faster than Hcy at physiological pH and it exists predominantly in the thiolate form. The isoelectric points of Hcy and Cys are 5.65 and 5.02, respectively.[9] Hence, both Hcy and Cys exist as negatively charged species at physiological pH. With Cu(II), Cys reacts faster than Hcy, resulting in the formation of a kinetically unstable 5-membered ring (as shown in Scheme S3, ESI†). The sulfhydryl group of Hcy deprotonates at a relatively slower rate than Cys. The deprotonated Hcy undergoes complexation with Cu(II) to form a kinetically favoured six membered ring. In both cases, a distinct fluorescence was initially observed upon addition of Hcy or Cys to the aqueous solutions of **1–4**. This could be presumably due to the reduction of Cu(II) to Cu(I), which subsequently disrupts the PET process causing restoration of the fluorescence intensity. Interestingly, the fluorescence intensity of the probe was dramatically quenched for Cys after 8 min incubation. Whereas, it reaches a plateau after 60 min incubation with Hcy (Fig. S25, ESI†). In case of Cys, the

unstable five membered ring is not kinetically favoured. Hence, following the decomplexation of Cys, Cu(I) quickly gets oxidized to Cu(II) by the dissolved oxygen in the medium.[10]

The electronic spectrum of **1** (Fig. 2a) displays a d–d band at 625 nm.[11] Upon addition of Hcy, the band disappeared suggesting the formation of Cu(I) species. Supplementary experimental evidence in support of the above mentioned redox mechanism is also revealed from EPR studies. As expected, in the absence of Hcy, **1** displayed a 4-line EPR spectrum with g values, $g_{\parallel}$ = 2.141 and $g_{\perp}$ = 2.044.[12] On addition of Hcy to **1**, EPR of the mixture turned silent (Fig. 2b). Clearly, the reduction of Cu(II) with Hcy is supported by EPR. Time dependent fluorescence of **1** with variable concentrations of Hcy/Cys was further explored to support the mechanism. Separate kinetic investigations of **1** with Hcy and Cys were performed at 7.4 pH. Following pseudo first order kinetics, the change in fluorescence intensity has been fitted against time following the equation mentioned in the literature.[13] Initial kinetic data of **1** (20 μM) with 500 μM Hcy/Cys is shown in Fig. S25 and S41 (ESI†). The observed rate constants (k_{obs}) are 0.039 and 1.73 min^{-1} for Hcy and Cys, respectively (Fig. S41–S43, ESI†). Clearly, the k_{obs} values hint at a faster reaction rate of Cys than Hcy, as already revealed in the earlier section. Interestingly, the short half-life ($t_{1/2}$) of Cys (0.40 min) further confirms the instability of the five membered ternary intermediate compared to the six membered conjugate with Hcy (**1**-Hcy adduct, $t_{1/2}$ = 17.77 min). The kinetic profile of **1** towards variable concentrations of Hcy was examined next (Fig. S42, ESI†). The observed rate constant (k_{obs}) values were calculated to be 0.039, 0.043, 0.082, and 0.204 min^{-1} for 500, 250, 100, and 50 μM Hcy, respectively (Fig. S43, ESI†). The $t_{1/2}$ values for 500, 250, 100 and 50 μM Hcy were found to be 17.77, 16.11, 8.45, and 3.4 min, respectively. The increase in the half-life value with a rise in the Hcy concentration undoubtedly confirms the kinetic stability of the intermediate at a higher concentration regime.

Finally, time correlated single photon counting (Fig. S44–S47, ESI†) showed a decrease in the fluorescence lifetime (τ) of **1** from 5.58 ns to 5.15 ns upon addition of Hcy (Table S5, ESI†). Radiative (k_r) and total non-radiative (k_{nr}) rate constants are given in Table S5 (ESI†). Higher k_{nr} values of **1–4** (Table S5, ESI†) presumably refer to the photoexcited electron transfer (PET) processes occurring in **1–4**.[14] This event has ultimately resulted in the low k_r values, which is reflected in the observed non-emissive nature of **1–4**. From Table S5 (ESI†), it is clear that the key factor for fluorescence enhancement of **1–4** with Hcy is k_r. Therefore, addition of Hcy to the probe's solution has resulted in the drop of the non-radiative deactivation pathway (*i.e.* quenching of the PET process).[14] As discussed earlier, binding of Hcy to Cu(II) reduces the metal center, which ultimately inhibits the PET process causing fluorescence enhancement of the probes with Hcy. In other words, reduction-induced-fluorescence-enhancement of the probes has resulted in the development of an optical method for the direct measurement of Hcy in aqueous samples.

Surprisingly, Hcy selective probes reported hitherto in the literature are not water-soluble. Table S1 (ESI†) seems to suggest that Hcy specific organic probes are hydrophobic in nature. However, metal complex derived probes are ionic, as described in this work and earlier by Li *et al.* Therefore, the ionic complexes would be a good choice for developing water-soluble probes.[2e] Validation and clinical testing of the probes are two key studies that are indispensable to ascertain the usability and prospects of the developed optical probes for biomedical research. Observation from Table S1 (ESI†) reveals that researchers have under-investigated this aspect while developing Hcy-specific probes. Herein, we sought to validate 1 with the HPLC method first. For this purpose, different concentrations of Hcy were derivatized with thiol selective UV labelling reagent.[15] A linear calibration plot (ranging 5–100 μM) was generated by plotting the ratio of peak area of Hcy to internal standard (IS) *versus* concentration of injected Hcy (Fig. 3a). A few representative chromatograms are shown in Fig. S48 and S49 (ESI†). To validate our assay, two unknown concentrations of Hcy were prepared from 100 μM stock solution. The concentrations of the unknown Hcy solutions were then measured by the fluorescence technique (Fig. 3b) using **1** as well as by the HPLC method (Fig. 3a). The experimentally measured values by both the techniques compare considerably with an error percentage of 2 (Table S6, ESI†). Hence, the results validates the optical sensor reported in this work.

To carry out the real-world application of **1** for early diagnostic drive, we tested **1** for direct measurement of Hcy in the blood plasma of a good number of cardiac patients. Retention of the 4 line EPR of **1** for more than half a day indicates the stability of the probe in blood plasma (Fig. S50, ESI†). Kinetic experiments were also performed in blood plasma (Fig. S51, ESI†). It reveals fluorescence regeneration of **1** on addition of Hcy to the quenched plasma sample. This implies the non-displacement of the Cu ion from iminocoumarin ligand even in blood plasma.

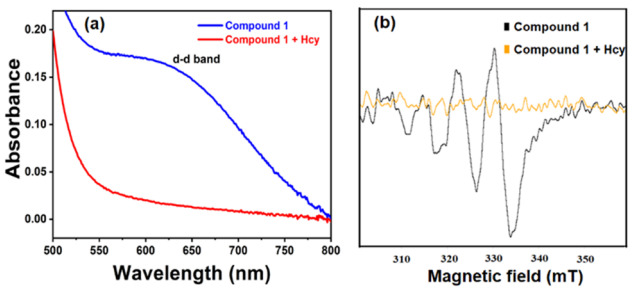

Fig. 2 (a) UV-vis spectra of **1** in the presence (blue line) and absence (red line) of Hcy (1 mM) in aqueous solution. (b) EPR spectra of **1** in the presence (black line) and absence (yellow line) of Hcy in an aqueous solution.

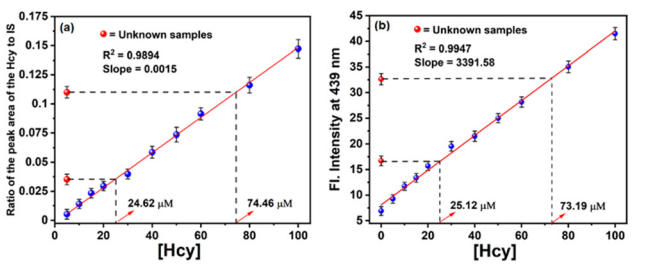

Fig. 3 Measurements of unknown concentrations of Hcy (a) using HPLC technique and (b) utilizing the linear fluorimetric calibration curve of **1** with Hcy in HEPES buffer solution (10 mM, pH = 7.4).

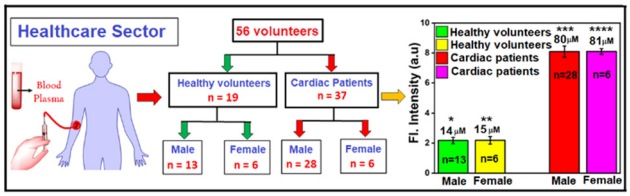

Fig. 4 Schematic representation showing Hcy levels measured by **1** in the blood samples of cardiac patients and healthy volunteers. In all cases (*, **, ***, and ****) $P < 0.05$. Each data point represents the average of triplicates.

Results from cytotoxicity studies of **1** and related Cu(I) species suggested no obvious toxicity (Fig. S52, ESI†). We next undertook the unique challenge of clinical investigation of **1**, which could be a potential candidate for point-of-care use. As expected, the fluorescence intensity of **1** was significantly lower in healthy volunteers than cardiac patients (Fig. 4). The total Hcy levels measured in the healthy volunteers were found to be in the range 09–17 μM and 10–16 μM in male and female categories, respectively. Meanwhile, the plasma tHcy levels in cardiac patients were calculated to be 70–82 μM and 74–80 μM in male and female samples, respectively (Fig. 4). The data presented in Fig. 4 indicates that the cardiac patients studied in this work have been suffering from intermediate hyperhomocysteinemia. Unprecedented clinical validation of our presented optical probe has also been performed by comparing the Hcy levels in a large number (sixty) of clinical samples. A clinically approved commercial immunoassay kit and current optical assay have been used to measure plasma tHcy levels in clinical samples. The results shown in Fig. S53 and Table S7 (ESI†) indicate that the Hcy level measured by the probe **1** compares reasonably well with the commercial kit. Thus, a simple and straightforward assay has been established in this work, which paves the way towards the possibility of the development of a miniature POCT kit for routine analysis and prognosis of various critical illnesses connected to HHcy in low resource settings.

In summary, we have reported herein a series of water soluble optical probes, which displayed a highly selective and interference-free turn-on fluorescence response towards homocysteine. EPR and UV-vis investigations provided evidence for the reduction-induced-emission-enhancement of the probes with Hcy. Validation of the presented optical assay has been performed by the traditional HPLC technique and reliability testing of **1** with regard to the clinically approved commercial immunoassay kit involving a large number of human plasma samples validates the simplicity and real-world application prospects of **1** as a novel molecular probe to measure the cardiac marker Hcy in patients' blood samples. Optical measurement of Hcy in human plasma samples using **1** and demonstration of its validation with sixty clinical samples is the first of its kind. The chemicals for preparing the probe and reagents required for the assay are inexpensive. Therefore, the present method reported herein demonstrates the feasibility for the development of a Hcy-selective diagnostic kit to be suitable for point-of-care testing.

This work is supported by the Govt. of India through the CSIR Grant no. MLP0047 and SERB (Grant no. CRG/2020/000577). SD and RRR acknowledge CSIR for their SRFs. The manuscript has CSIR-CSMCRI registration number 161/2021. Prior consent was obtained from human subjects.

Conflicts of interest

The authors declare no conflict of interest.

Notes and references

1 (*a*) G. E. Lonn, S. Yusuf, M. J. Arnold, P. Sheridan, J. Pogue, M. Micks, J. Probstfield, G. Fodor, C. Held and J. J. Genest, *N. Engl. J. Med.*, 2006, **354**, 1567–1577; (*b*) S. Seshadri, A. Beiser, J. Selhub, P. F. Jacques, I. H. Rosenberg, R. B. D'Agostino, P. W. F. Wilson and P. A. Wolf, *N. Engl. J. Med.*, 2002, **346**, 476–483; (*c*) H. Refsum and P. M. Ueland, *Annu. Rev. Med.*, 1998, **49**, 31–62; (*d*) M. Sibrian-Vazquez, J. O. Escobedo, S. Lim, G. K. Samoei and R. M. Strongin, *Proc. Natl. Acad. Sci. U. S. A.*, 2010, **107**, 551–554.
2 (*a*) W. Wang, J. O. Escobedo, C. M. Lawrence and R. M. Strongin, *J. Am. Chem. Soc.*, 2004, **126**, 3400–3401; (*b*) X. Yang, Y. Guo and R. M. Strongin, *Angew. Chem., Int. Ed.*, 2011, **50**, 10690–10693; (*c*) H. Peng, K. Wang, C. Dai, S. Williamson and B. Wang, *Chem. Commun.*, 2014, **50**, 13668–13671; (*d*) H. Y. Lee, Y. P. Choi, S. Kim, T. Yoon, Z. Guo, S. Lee, K. M. K. Swamy, G. Kim, J. Y. Lee, I. Shin and J. Yoon, *Chem. Commun.*, 2014, **50**, 6967–6969; (*e*) Z. Li, Z. R. Geng, C. Zhang, X. B. Wang and Z. L. Wang, *Biosens. Bioelectron.*, 2015, **72**, 1–9; (*f*) J. Wang, Y. Liu, M. Jiang, Y. Li, L. Xia and P. Wu, *Chem. Commun.*, 2018, **54**, 1004–1007; (*g*) J. O. Escobedo, W. Wang and R. M. Strongin, *Nat. Protoc.*, 2007, **1**, 2759–2762.
3 C. X. Yin, K. M. Xiong, F. J. Huo, J. C. Salamanca and R. M. Strongin, *Angew. Chem., Int. Ed.*, 2017, **56**, 13188–13198.
4 R. R. Nair, M. Raju, K. Jana, D. Mondal, E. Suresh, B. Ganguly and P. B. Chatterjee, *Chem. – Eur. J.*, 2018, **24**, 10721–10731.
5 D. Cao, Z. Liu, P. Verwilst, S. Koo, P. Jangjili, J. S. Kim and W. Lin, *Chem. Rev.*, 2019, **119**, 10403–10519.
6 D. Ray and P. K. Bharadwaj, *Inorg. Chem.*, 2018, **47**, 2252–2254.
7 H. Sung Jung, J. Hye Han, Y. Habata, C. Kang and J. Seung Kim, *Chem. Commun.*, 2011, **47**, 5142–5144.
8 U. Reddy, H. Agarwalla, N. Taye, S. Ghorai, S. Chattopadhyay and A. Das, *Chem. Commun.*, 2014, **50**, 9899–9902.
9 Q. Ma, X. Fang, J. Zhang, L. Zhu, X. Rao, Q. Lu, Z. Sun, H. Yu and Q. Zhang, *J. Mater. Chem. B*, 2020, **8**, 4039–4045.
10 D. Chao and Y. Zhang, *Sens. Actuators, B*, 2017, **245**, 146–155.
11 E. Faggi, R. Gavara, M. Bolte, L. Fajarí, L. Juliá, L. Rodríguez and I. Alfonso, *Dalton Trans.*, 2015, **44**, 12700–12710.
12 E. Garribba and G. Micera, *J. Chem. Educ.*, 2006, **83**, 1229–1232.
13 X. F. Yang, Q. Huang, Y. Zhong, Z. Li, H. Li, M. Lowry, J. O. Escobedo and R. M. Strongin, *Chem. Sci.*, 2014, **5**, 2177–2183.
14 R. R. Nair, S. Debnath, S. Das, P. Wakchaure, B. Ganguly and P. B. Chatterjee, *ACS Appl. Bio Mater.*, 2019, **2**, 2374–2387.
15 E. Bald, E. Kaniowska, G. Chwatko and R. Glowacki, *Talanta*, 2000, **50**, 1233–1243.